Journal of Saudi Chemical Society (2023) 27, 101619

King Saud University

Journal of Saudi Chemical Society

www.ksu.edu.sa
www.sciencedirect.com

ORIGINAL ARTICLE

Spectroscopic, anti-bacterial, anti-cancer and molecular docking of Pd(II) and Pt(II) complexes with (E)-4-((dimethylamino)methyl)-2-((4,5-dimethylthiazol-2-yl)diazenyl)phenol ligand

Ahmed S.M. Al-Janabi [a,*], Khulood H. Oudah [b], Samar A. Aldossari [c], Mohamed A. Khalaf [d], Abdulrahman M. Saleh [e], Mohammad R. Hatshan [c], Nourah B. Altheeb [c], Syed Farooq Adil [c,*]

[a] *Department of Chemistry, College of Science, Tikrit University, Tikrit, Iraq*
[b] *Pharmaceutical Chemistry Department, College of Pharmacy, Al-Ayen University, Thi-Qar, Iraq*
[c] *Department of Chemistry, College of Science, King Saud University, P.O. Box 2455, Riyadh 11451, Saudi Arabia*
[d] *Department of Chemistry, College of Science, United Arab Emirates University, P. O. Box 15551, Al Ain, United Arab Emirates*
[e] *Pharmaceutical Medicinal Chemistry & Drug Design Department, Faculty of Pharmacy (Boys), Al-Azhar University, Cairo 11884, Egypt*

Received 30 November 2022; revised 15 February 2023; accepted 18 February 2023
Available online 23 February 2023

KEYWORDS

Azo dye;
Thiazole;
Biological activity;
Molecular docking;
Palladium;
Platinum

Abstract New ligand (*E*)-4-((dimethylamino)methyl)-2-((4,5-dimethylthiazol-2-yl)diazenyl)phenol (HDmazo) was prepared by the coupling reaction between 4,5-dimethylthiazol-2-amine and 4-((dimethylamino)methyl)phenol. Moreover, the $[MCl_2(HDmazo)]$ and $[M(HDmazo)_2]$ [M^{II} = Pd and Pt] were prepared using the direct reaction of equivalent molar of HDmazo and Na_2PdCl_4 or K_2PtCl_4. The HDmazo and its complexes were investigated by different spectroscopic techniques. In complexes (**1**–**2**) HDmazo ligand behaves as bidentate style through the nitrogen of azo group and nitrogen of thiazole ring towards Pd(II) and Pt(II). Or in a bidentate fashion via the oxygen atom of the hydroxylate group and nitrogen atom of azo group as mono-anion in complexes (**3**–**4**). Further, the study of biological activity against four pathogenic bacteria showed that compound (**3**) exhibited good activity compared to other compounds. Additional the anti-tumor action against A2870 cell lines was screened, and the complexes (**1**) and (**2**) displayed good activity

* Corresponding authors.
E-mail address: sfadil@ksu.edu.sa (S. Farooq Adil).
Peer review under responsibility of King Saud University. Production and hosting by Elsevier.

Production and hosting by Elsevier

https://doi.org/10.1016/j.jscs.2023.101619

with 7.45 ± 0.98 μM and 13.23 ± 1.43 μM, respectively. The binding mechanism of the prepared compounds with EGFR tyrosine kinase, was investigated using molecular docking experiments.

1. Introduction

In our daily lives, heterocyclic compounds are extremely interesting. Any number of hetero-atoms can be found in a heterocyclic compound. The most prevalent hetero-cycles are those with five or six members and include hetero-atoms of sulfur, oxygen, or nitrogen. Simple heterocyclic compounds such as pyrimidine, pyrrolidine, pyrroles, and thiophene are well-known examples [1].

The azo dyes have good stability and strong dyeing strength qualities, which are used in many different fields. They have a molecular structure, nonlinear optics, antibacterial activity, and absorption characteristics. The inquiry into the cutting-edge molecular optical characteristics of the azo dyes has been documented in the literature [2]. In the last many decades, the synthesis and characterization of many azo dyes containing thiazole rings in a structure such as 2-[2′-(5-nitrothiazolyl)azo]-4-methoxyphenol [3], 2-[2′-(6-methoxy benzothiazolyl)azo]-4-ethoxyphenol [4], 2-[2- (4,5-Dimethyl thiazolyl)azo]- 4-methoxy phenol [5], 4-methyl-5-(4-acetylphenyldiazenyl)thiazol-2-amine [6], etc. [6–10]. The development of coordination chemistry has benefited greatly by the use of azo dyes with thiazole rings [2]. These substances are useful because they have a wide range of uses in biological, electrochemical, and analytical research [11–17]. Due to their potential for cytotoxicity, antibacterial, antimycobacterial, and antioxidant properties, the complexes of divalent ions with heterocyclic ligands containing S and N atoms have been widely studied [11–18].

In this work, we describe the preparation and identification of the azo ligand (*E*)-4-((dimethylamino)methyl)-2-((4,5-dimethylthiazol-2-yl)diazenyl)phenol and complexation with palladium(II) and platinum (II) ions. The HDmazo and its complexes were examined against the bacteria *Escherichia coli*, *staphylococcus aureus*, *Klebsiella pneumoniae* and *Pseudomonas aeruginosa*. In addition, we studied the interactions established between the EGFR tyrosine kinase and prepared compounds using molecular docking.

2. Experimental part

2.1. Material and instruments

All chemicals and solvents were purchased from commercial vendors such as Fluke, BDH, and Aldrich and used without purification. Uncorrected melting points were measured using a Gallenkamp melting point instrument. In the 400–4000 cm^{-1} range of the Shimadzu FT-IR 8400 spectrophotometer was used to record the IR spectra (in KBr disk). NMR spectra were recorded (DMSO d_6) on a JEOL resonance (500 MHz) NMR spectrometer using TMS as an internal standard. CHN analysis was recoded using thermo-GS 352 apparatus.

2.2. Synthesis of (E)-4-((dimethylamino) methyl)-2-((4, 5-dimethylthiazol-2-yl)diazenyl)phenol (HDmazo)

The azo dye ligand was prepared and isolated in similar method describe by A. S. Waheeb et al. [8] using coupling reaction between 4,5-dimethylthiazol-2-amine and 4-((dimethylamino)methyl)phenol in equivalent molar.

HDmazo: Bright yellow solid. Yield: 79 %. Anal. calc. for $C_{14}H_{18}N_4OS$: C, 57.91; H, 6.25; N, 19.29. Found: C, 58.11; H, 6.31; N, 19.41 %. IR (KBr): 3357 ν(O—H); 3080, 3039 ν(C—H $_{aromatic}$); 2960, 2891ν(C—H $_{aliphatic}$); 1623 ν(C═N $_{thiazole\ ring}$); 1568ν(C═C); 1496ν(N═N); 1353ν(CH_3 $_{bending,\ rock}$); 1244ν(C—N);1182ν(CH_3 $_{wag}$); 750ν(oop C—H $_{bending}$) cm^{-1}. ^{1}H NMR (DMSO d_6): δ 2.09(s, 6H, CH_3 **13**,**13′**), 2.29(s, 3H, CH_3**10**), 2.55(s, 3H, CH_3**11**), 3.76(s, 2H, CH_2**12**), 7.36(d, 1H, *J* 8.00 Hz, **H5**), 7.46(d, 1H, *J* 8.00 Hz, **H6**), 7.62(s, 1H, **H3**), 9.94(s, 1H, **OH**).ppm. Melting point: 189–192 °C.

2.3. Synthesis of [$PdCl_2$(HDmazo)](1)

An ethanolic solution of (E)-4-((dimethylamino)methyl)-2-((4,5-dimethylthiazol −2-yl)diazenyl)phenol (HDmazo) (0.150 g, 0.517 mmol) in (20 ml) was added to a solution of Na_2PdCl_4 (0.152 g, 0.517 mmol) in distal water (10 ml), in round bottom flask (50 ml), with stirring. The color of mixture was changed to bright brown. The mixture was refluxed for 5 h, then a bright brown ppt was formed, then filtered off, washed in several time with distal water and ethanol and dried under vacuum. The product was recrystallized from DMSO/EtOH.The [$PtCl_2$(HDmazo)](**2**) complex was prepared and isolated in similar method describe above.

2.3.1. [$PdCl_2$(HDmazo)] (**1**)

Bright brown solid. Yield: 0.237 g, 87 %. Anal. calc. for $C_{14}H_{18}Cl_2N_4OPdS$: C, 35.95; H, 3.88; N, 11.98. Found: C, 36.08; H, 4.29; N, 12.24 %. Molar conductivity in DMSO: 11.32 (Ω^{-1} cm^{-1} mol^{-1}). IR (KBr); 3413 ν(O—H); 3014 ν(C—H $_{aromatic}$); 2942ν(C—H $_{aliphatic}$); 1587 ν(C═N $_{thiazole\ ring}$); 1544ν(C═C); 1460ν(N═N); 1353ν(CH_3 $_{bending\ (rock)}$); 1242ν(C—N);1197ν(CH_3 $_{wag}$); 740ν(oop C—H $_{bending}$), 443ν(Pd-N). ^{1}H NMR (DMSO d_6): δ 2.10(s, 6H, CH_3 **13**,**13′**), 2.30(s, 3H, CH_3**10**), 2.58(s, 3H, CH_3**11**), 3.90(s, 2H, CH_2**12**), 7.35(d, 1H, *J* 8.00 Hz, **H5**), 7.45(d, 1H, *J* 8.00 Hz, **H6**), 7.62(s, 1H, **H3**), 9.87(s, 1H, **OH**). ppm. Melting point: 273–275 °C.

2.3.2. [$PtCl_2$(HDmazo)] (**2**)

Reddish yellow solid. Yield: 0.214 g, 80 %. Anal. calc. for $C_{14}H_{18}Cl_2N_4OPtS$: C, 30.22; H, 3.26; N, 10.07. Found: C, 30.41; H, 3.37; N, 10.30 %. Molar conductivity in DMSO: 16.71 (Ω^{-1} cm^{-1} mol^{-1}). IR (KBr); 3413 ν(O—H); 3014 ν(C—H $_{aromatic}$); 2921, 2823 ν(C—H $_{aliphatic}$); 1582 ν

(C═N $_{thiazole\ ring}$); 1544ν(C═C); 1460ν(N═N); 1353ν(CH_3 $_{bending\ (rock)}$); 1242ν(C—N);1197ν(CH_3 $_{wag}$); 740ν(oop C—H $_{bending}$), 441ν(Pt-N) cm^{-1}. ^1H NMR (DMSO d_6): δ 2.02(s, 6H, CH_3 **13**,**13′**), 2.24(s, 3H, CH_3**10**), 2.71(s, 3H, CH_3**11**), 3.80(s, 2H, CH_2**12**), 7.42(d, 1H, *J* 8.00 Hz, **H5**), 7.52(d, 1H, *J* 8.00 Hz, **H6**), 7.72(s, 1H, **H3**), 10.13(s, 1H, **OH**). ppm. Melting point: 203–205 °C.

2.4. Synthesis of [Pd(Dmazo)$_2$](3)

An ethanolic solution of (E)-4-((dimethylamino)methyl)-2-((4,5-dimethylthiazol −2-yl)diazenyl)phenol (HDmazo) (0.300 g, 1.124 mmol) in (20 ml) containing some drops of Et_3N as a base, was added to an aqueous solution of Na_2PdCl_4 (0.152 g, 0.517 mmol) in (10 ml), with stirring. A reddish brown ppt was formed directly. The combination was stirred for 3 h, then the ppt afforded was filtered off, washed several times with distal water and ethanol, and dried under vacuum. The product was recrystallized from DMSO/EtOH. The [Pt(Dmazo)$_2$](**4**) complex was prepared and isolated in a similar method described above.

2.4.1. [Pd(Dmazo)$_2$] (**3**)

Dark brown solid. Yield: 0.178 g, 91 %. Anal. calc. for $C_{28}H_{34}N_8O_2PdS_2$: C, 49.08; H, 5.00; N, 16.35. Found: C, 49.03; H, 5.25; N, 16.42 %. Molar conductivity in DMSO: 10.07 (Ω^{-1} cm^{-1} mol^{-1}). IR (KBr); 3060 ν(C—H $_{aromatic}$); 2921 ν(C—H $_{aliphatic}$); 1595 ν(C═N $_{thiazole\ ring}$); 1544ν(C═C); 1452ν(N═N); 1350ν(CH_3 $_{bending\ (rock)}$); 1238ν(C—N);1188ν(CH_3 $_{wag}$); 763ν(oop C—H $_{bending}$), 551ν(Pd-O); 441 ν(Pd-N) cm^{-1}. ^1H NMR (DMSO d_6): δ 2.09(s, 6H, CH_3 **13**,**13′**), 2.29(s, 3H, CH_3**10**), 2.64(s, 3H, CH_3**11**), 3.87(s, 2H, CH_2**12**), 7.44–7.62 (*m*, 3H, *J* 8.00 Hz, **H3,5,6**). ppm. Melting point: 256–258 °C.

2.4.2. [Pt(Dmazo)$_2$] (**4**)

Dark brown solid. Yield: 0.159 g, 79 %. Anal. calc. for $C_{28}H_{34}N_8O_2PtS_2$: C, 43.46; H, 4.43; N, 14.48. Found: C, 43.51; H, 4.69; N, 14.63 %. Molar conductivity in DMSO: 14.23 (Ω^{-1} cm^{-1} mol^{-1}). IR (KBr); 3060 ν(C—H $_{aromatic}$); 2921 ν(C—H $_{aliphatic}$); 1595 ν(C═N $_{thiazole\ ring}$); 1544ν(C═C); 1452ν(N═N); 1350ν(CH_3 $_{bending\ (rock)}$); 1238ν(C—N);1188ν(CH_3 $_{wag}$); 763ν(oop C—H $_{bending}$), 548ν(Pd-O); 437 ν(Pd-N) cm^{-1}. ^1H NMR (DMSO d_6): δ 2.14(s, 6H, CH_3 **13**,**13′**), 2.36(s, 3H, CH_3**10**), 2.71(s, 3H, CH_3**11**), 3.86(s, 2H, CH_2**12**), 7.23–7.72 (*m*, 3H, *J* 8.00 Hz, **H3,5,6**). ppm. Melting point: 281–282 °C.

2.5. Anti-bacterial studies

The anti-bacterial activity study of azo dye ligand and their complexes were screened against *Escherichia coli*, *staphylococcus aureus*, *Klebsiella pneumoniae* and *Pseudomonas aeruginosa* by diffusion method agar describe by Baurer et al. [19] in 10^{-3} M of DMSO solution, and the results were compared with gentamicin as the positive control and DMSO as negative control. Then, the established inhibition zone was measured. The activities of the azo dye ligand and its complexes were established by calculating the activity index (AI).

Also the free ligand and its complexes were examined against *similar pathogenic bacteria* to calculate the minimal inhibitory concentrations (MIC) using a micro-dilution method describe by Baurer et al. [19]. The study was carried out on Muller-Hinton agar (37 °C, 24 h). The compounds (10, 20, 40, 80, 100, 150, 200, 400 μg/mL) were examined for antimicrobial activity against the bacterial species. Gentamicin and Amoxicillin were used as standard for comparison of antibacterial activity under similar conditions.

2.6. Anti-cancer studies

The anti-tumor activity of free ligand (**LH**) and their complexes (**1**–**4**) were examined against human liver carcinoma cells (HepG-2) and breast carcinoma cells (MCF-7) by procedures describe by Tan et al. [20] using a 3.5×10^3 and 2.8×10^3 cells for (**MCF-7**) and (**A569**). The viability-percentage was premeditated, and the IC_{50} value was recorded by plotting the percentage viability against the concentration of the test compound on a logarithmic scale using the Graph-Pad Prism 9 software.

2.7. Molecular docking

The molecular docking study was done private the pockets of (EGFR tyrosine kinase) by using MOE 19.0901 Software. The binding site was operated, within crystal protein (PDB codes: 4HJO) (https://www.rcsb.org). At first, water molecules and unnecessary atoms were removed then minimization was done to give our protein the best conformation. The tested compounds were generated and drawn by Chem-draw 2017 software. Then the molecules were ready after doing the quick preparation option. Docking was done and all results were collected in Table 4 containing affinity scores of our compounds against EGFR tyrosine kinase.

3. Result and discussion

3.1. Synthesis

Treatment equivalent molar of ethanolic solution of (*E*)-4-((dimethylamino)methyl)-2-((4,5-dimethylthiazol-2-yl)diazenyl)phenol ligand (HDmazo) with an aqueous solution of **s**odium tetrachloro palladate(II) or potassium tetrachloro platinate (II) (Scheme 1), afford complexes of the following type [MCl_2(-HDmazo)] [where M^{II} = Pd (**1**) or Pt (**2**)]. The results suggest that the HDmazo ligand behaves as bidentate style through the nitrogen of azo group and nitrogen of thiazole ring towards Pd (II) or Pt(II) to afford square planner around metal ions with two chloride ions.

Whereas the treatment two equivalents of azo ligand (HDmazo) with one equivalent of Na_2PdCl_4 or K_2PtCl_4 salts in present KOH as a base gave [M(Dmazo)$_2$]complexes (**3**,**4**) (Scheme 2), the results indicated that the anion ligand ($Dmzao^-$) acts as bidentate fashion through the oxygen atom of hydroxyl group and nitrogen atom of azo group to produce a square planer geometry around metal ions. The synthesized complexes were investigated using CHN analysis, IR, NMR,

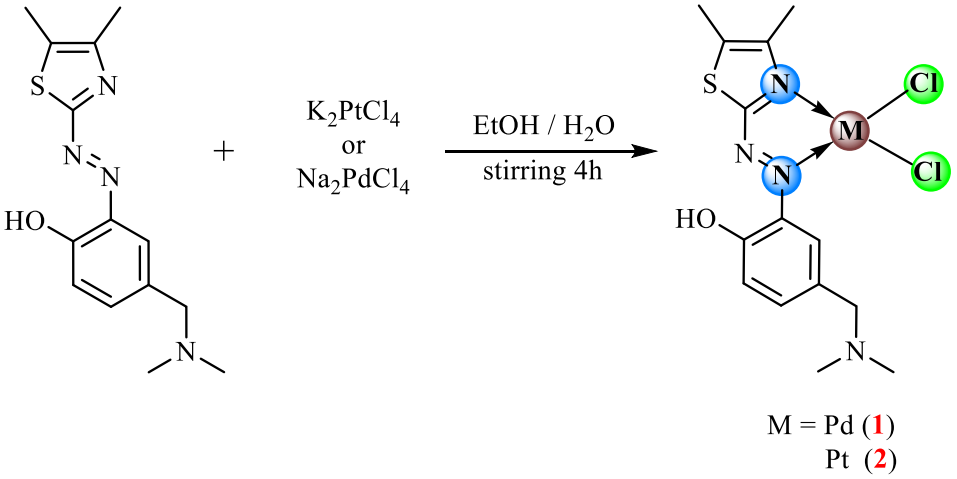

Scheme 1 Preparation of complexes (**1**, **2**).

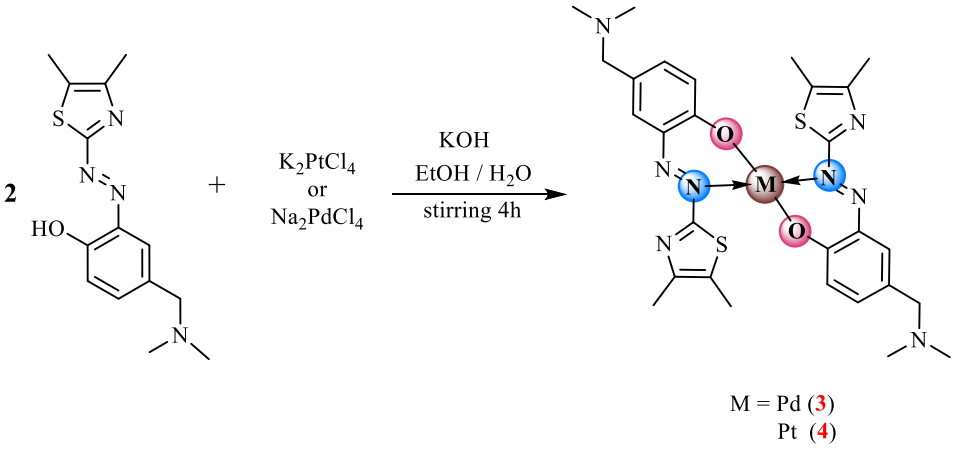

Scheme 2 Preparation of complexes (**3**, **4**).

mass spectroscopy, and molar conductivity measurements are listed in the experimental section.

3.2. Mass spectrum of HDmazo ligand

The mass spectrum of the 3(*E*)-4-((dimethylamino)methyl)-2-((4,5-dimethylthiazol-2-yl)diazenyl)phenol ligand (Fig. 1) shows the peak which represents the commonest fragment ion to be formed for the HDmazo ligand (m/z = 290.4), $C_{14}H_{18}N_4OS$ (m/z: 290.12)(This peak due to the **HDmazo** ligand), $C_{14}H_{17}N_4S^{\bullet}$ (m/z = 274.12), $C_{11}H_{10}N_3OS^{\bullet}$ (m/z = 233.05), $C_9H_{12}N_3O^{\bullet}$ (m/z = 174.10), $C_9H_{12}N_2O^{2\bullet}$ (m/z = 164.09), $C_9H_{12}NO^{\bullet}$ (m/z = 150.09), $C_5H_6N_2S^{2\bullet}$ (m/z = 126.03), $C_6H_4N_2O^{2\bullet}$ (m/z = 120.03), $C_6H_5^{\bullet}$ (m/z: 77.04) (Scheme 3). The mass spectra of the [$PdCl_2$(HDmazo)](**1**) and [$PtCl_2$(HDmazo)](**2**) showed the main fragment peaks for these complexes. The molecular weight of complex (**1**) is (467.71 g/mol) was assigned to the base m/z ($C_{14}H_{18}Cl_2N_4OPdS$) = 468.4 peak (**Figure S1**). While the molecular weight of complex (**2**) is (556.37 g/mol) and the peak at m/z ($C_{14}H_{18}Cl_2N_4OPtS$) = 557.9 which represented to this complex (**Figure S2**).

3.3. IR spectra

The infrared spectrum of the azo-derivative ligand (**Figure S3**) showed four distinct bands, which belong to ν(OH), ν(C═N)$_{thiazole}$, ν(N═N), and ν(C─N) at 3357 cm^{-1}, 1623 cm^{-1}, 1496 $cm^{-1}$and 1244 cm^{-1}, respectively. This enhanced the formation of azo derivative due to the disappearance of νNH_2 of amine and appeared of a band (N═N) that was not present in the IR spectrum of the 4-((dimethylamino) methyl)phenol. Also, the infrared spectra showed the ν(C─H) stretching of the aliphatic and aromatic groups within the range (2891–3080) cm^{-1}.

The comparison of IR data of the [MCl_2(HDmazo)] [where M^{II} = Pd (**1**) or Pt (**2**)] (**Figure S4**) with IR of free ligand designated after over a shift of the distinguishing bands of the functional groups included in the bonding to the ion. Broad-band shown in IR spectra of the complexes at 3413 cm^{-1} for the complexes assigned to the ν(O─H), the slightly shifted of this band compared with that of free ligand, indicating that O─H group doesn't participate in bonding [21–22]. The stretching of the ν (N═N) group has shifted towards lower

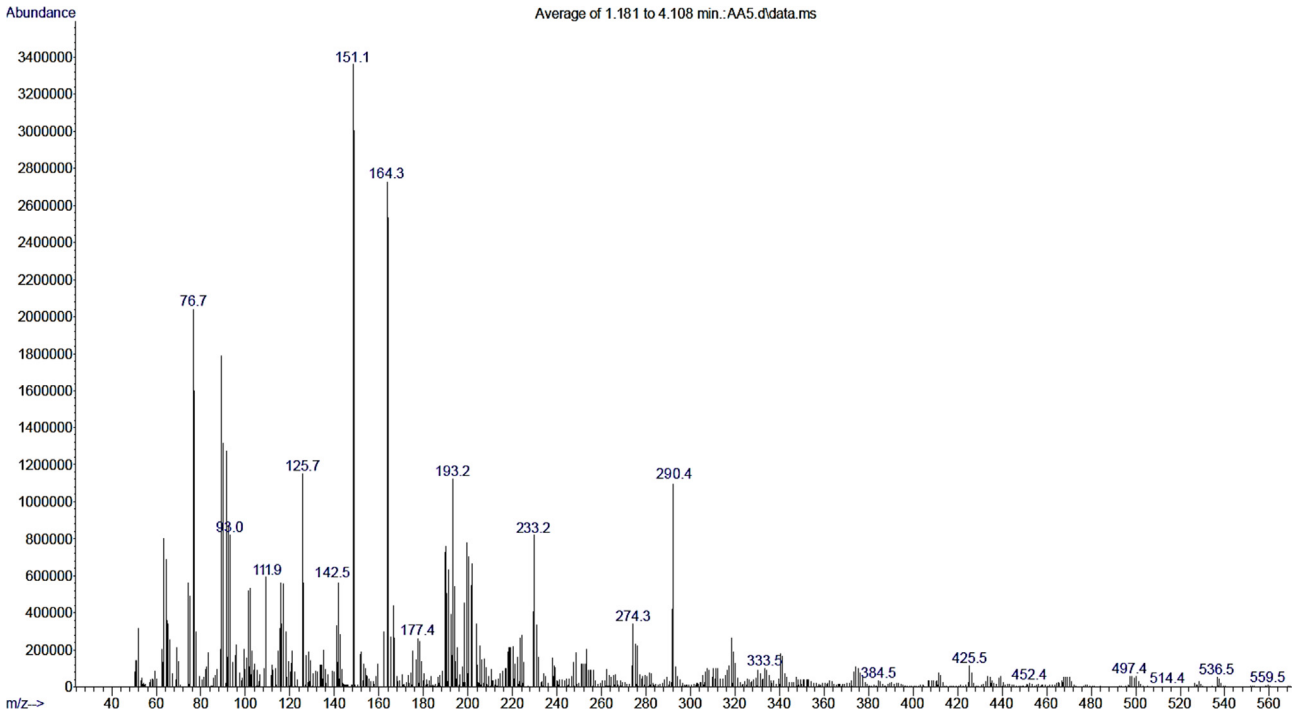

Fig. 1 Mass spectrum of HDmazo ligand.

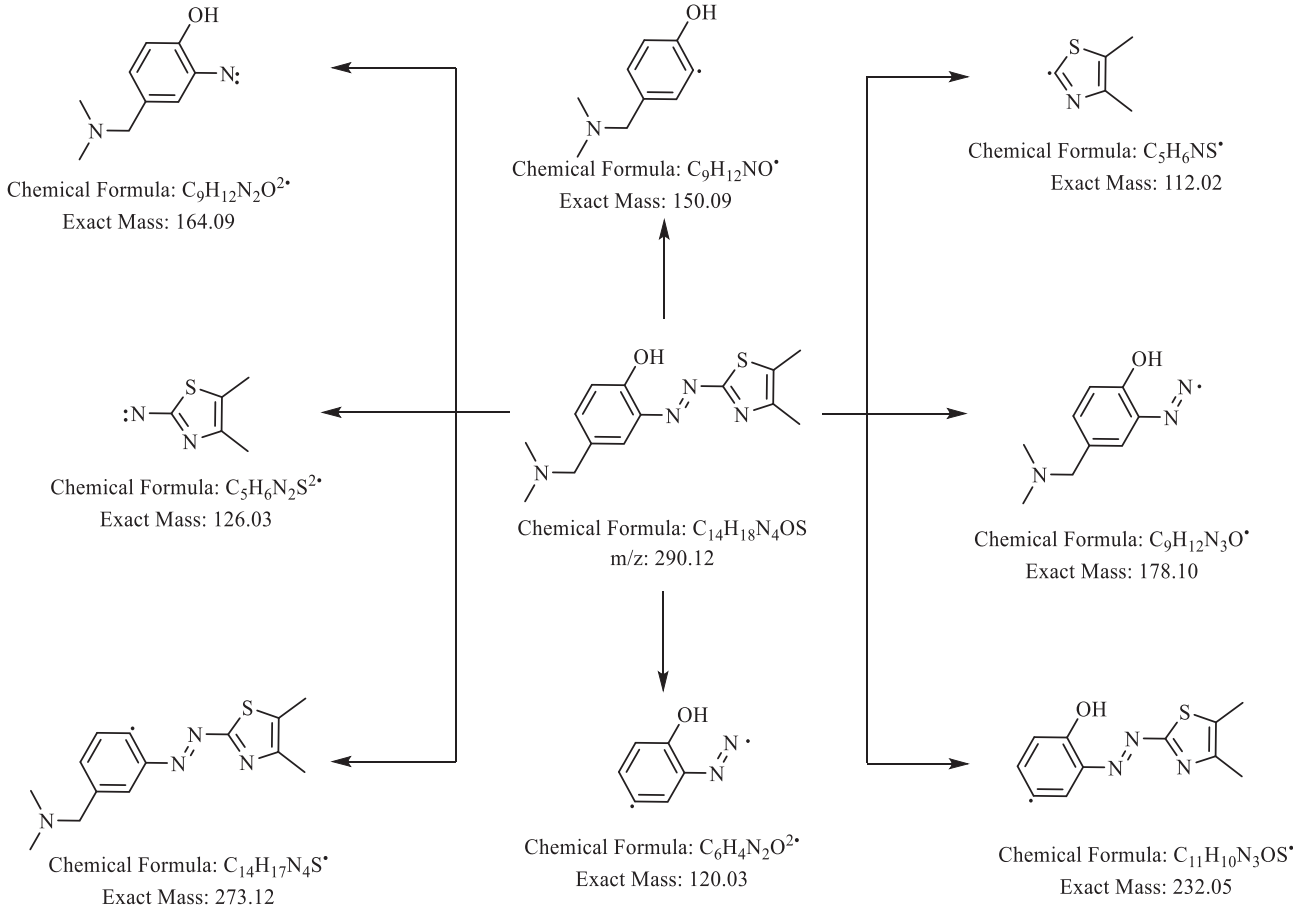

Scheme 3 The fragmentation pattern of HDmazo ligand.

frequencies than in the free ligand (1623) cm^{-1}, and this indicates the coordination of the ligand with ions via nitrogen atom [23–24], and also a shift in the stretching frequency of ν(C═N) (which showed at 1587 and 1582 cm^{-1}) compared to its value in ligand, and this indicates the consistency of the ligand with metals through nitrogen atom [25–29].

It is noticed through the IR spectra of complexes (**3**) and (**4**) (**Figure S5 and S6**) disappearance the frequencies of the OH group band that was appearing in the HDmazo free at (3357) cm^{-1}, which enhances the deprotonation and coordinating with the ions through the oxygen of hydroxylate group as an anion, The involvement of this group in complex formation is apparent from the redshift of νC-O due to C—O—M bond formation [21–22,30–32]. The frequency of the azo group ν(-N═N-) was shifted to lower frequencies compared to its value in the free ligand, and this indicates the coordinated through the nitrogen atom of the azo group. As well as the IR spectra displayed new bands that were not present in the spectrum of free ligand at (441, 437) and (545, 548) cm^{-1} attributed to the ν(M−O) and ν(M−N), respectively. This indicates the bonding of the metal with the ligand through nitrogen and oxygen atoms [24–29,33].

3.4. NMR spectra

The ^{1}H NMR spectrum of the HDmazo ligand (**Figure S7**) showed four singlet peaks in the shielding area at δH = 2.09 ppm, 2.29 ppm, 2.55 ppm, and 3.76 ppm attributed to the protons three methyl groups and one methylene group respectively, and its integration indicates that it corresponds to the number of protons. Whereas the protons of the phenyl ring are displayed as three separated peaks at δH = 7.36 ppm (d, H5), 7.46 ppm (d, H6), and 7.62 ppm (s, H3). The complementarity of each of the three peaks of the phenyl ring indicates that they correspond to one proton. Also, the spectrum showed the proton of the hydroxyl group at δH = 9.94 ppm. This peak is showed in the ^{1}H NMR spectra of complexes (**1**) and (**2**) at δH = 9.87 ppm, and 10.13 ppm, the slightly shifted of this peak compared with that of free ligand, indicating that O—H group doesn't participate in bonding with metal ions(**Figure S8**). While this peak was disappearance in the in the ^{1}H NMR spectra of complexes (**3**) and (**4**) (**Figure S9 and S10**), which enhances the deprotonation and coordinating with the ions through the oxygen of hydroxylate group as an anion. The protons of methyl and methylene group exhibited in similar position or slightly shift compared with free ligand. The chemical shifts of the azo dye ligand and its complexes are listed in the experimental section.

The ^{13}C–^{1}H NMR spectrum of the HDmazo (Fig. 2) displayed the chemical shifts of carbons of methyl groups C10, C11, C13 and C12 at δC = 16.01 ppm, 24.30 ppm, 49.06 ppm, and 66.25 ppm respectively. The carbons of phenyl rings and thiazole ring showed within δC = 125.06 – 166.86 ppm.

3.5. Anti-bacterial studies

The development of novel bacterial strains that are resistant to modern antibiotics is a serious issue for public health. Therefore, it's important to discover substitute substances that have drug-like properties. Recently, scientists have examined the production of novel metal complexes with novel chemical ligands and evaluated their antibacterial efficacy.

In this study, we measured the diameter inhibition zone (DIZ), and activity index of the tested compounds against *S. aureus*, *E.coli*, *K. pneumoniae* and *P. aeruginosa*, in compared with gentamicin as positive control and DMSO (the solvent) as negative control (which no antimicrobial properties by itself) (Table 1). The activity index (A.I.) values of the synthesized comps were calculated affording to the following equation:

$$\text{Activity index}\,(\%) = \frac{\text{Inhibition zone of compound}}{\text{Inhibition zone of standard}} * 100\%$$

The results indicated that azo dye ligand and its complexes (**1**–**4**) have good activity against the pathogenic bacteria, and their activity was in the following order:

(**3**) > (**1**) > (**2**) > (**4**) > HDmazo

The palladium complexes have a stronger antibacterial behavior against all pathogenic bacteria compared with free ligand and platinum complexes. Further, the [$Pd(Dmazo)_2$] (**3**) showed a highest activity than the other compounds. Additional, this complex has a highest towards *Escherichia coli* as well as *Staphylococcus aureus* that other bacteria species.

There are two possibilities that might account for this expansion in complex activity:

(1) The overtone idea [34] holds that an antibacterial compound's solubility in the lipids that make up the cell membrane, which only allows the passage of soluble components, has a considerable impact on its antibacterial effectiveness.
(2) Tweedy's chelation hypothesis [35], which describes how a metal ion's polarity can be greatly reduced by the orbital overlap of the ligand and the positive charge division of the core metallic ion with the donor atoms of the ligand.

The results showed in Fig. 3, which indicated that the [$Pd(Dmazo)_2$] (**3**) complex has the highest activity index, whereas the HDmazo has a lowest activity index.

In addition the minimum inhibition concentration of the (*E*)-4-((dimethylamino)methyl)-2-((4,5-dimethylthiazol-2-yl)diazenyl)phenol ligand and its complexes were examined against four bacteria species, using a micro-dilution method. The antibacterial activity of prepared compounds was moderate to good, with MIC ranging from 10 to 400 μg/mL, and the results are recorded in Table 2. The prepared complexes showed good activity and are equal or more activity than the Amoxicillin drug, but lowest than Gentamicin drug. The order of activity can be presented as follows:

(**2**) > (**1**) > (**3**) > (**4**) > HDmazo

The best activity was achieved for complex (**1**) with MIC 80 and 100 μg/mL, for the four bacterial species respectively. Whereas the complex (**4**) and free ligand displayed a lowest activity against pathogenic bacteria. Other results are listed in Table 1.

3.6. Cytotoxicity studies

The second biggest cause of death worldwide in the twenty-first century is cancer. According to the American Cancer Soci-

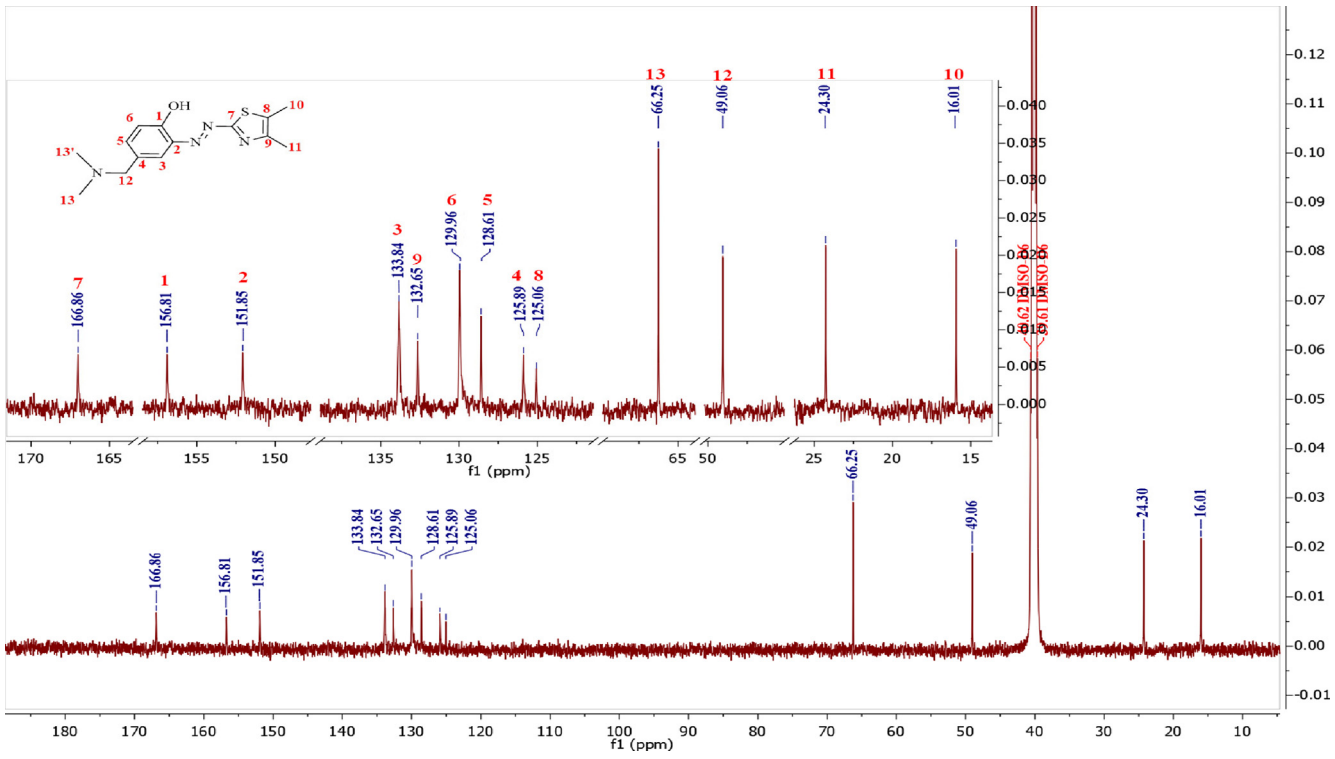

Fig. 2 ^{13}C NMR spectrum of HDmazo ligand.

Table 1 Diameter inhibition zone (DIZ in mm) and activity index (A.I. in %) of the synthesized compounds.

Seq.	*S. aureus*		*P. aeruginosa*		*K. pneumoniae*		*E.Coli*	
	DIZ	A.I.	DIZ	A.I.	DIZ	A.I.	DIZ	A.I.
HDmazo	18	62	14	47	11	44	19	61
1	23	79	21	70	16	64	23	74
2	20	69	19	63	15	60	20	65
3	25	86	23	77	19	76	27	87
4	21	72	21	70	16	64	22	71
Gentamicin	29	100	30	100	25	100	31	100

ety Cancer Facts & Figures 2020 [36], compared to other diseases, cancer accounts for about one out of every-six fatalities globally. Numerous anticancer drugs are already available on the market, but their widespread usage has been constrained by issues such as toxicity, adverse effects, limited effectiveness, non-specificity, and low water solubility [37]. In order to put an end to the cancer ghost, there is a constant need for the creation of new and promising cancer chemotherapeutic treatments [38–39].

Thus, the in vitro cytotoxic effects of the new azo dye ligand and its Pd(II) and Pt(II) complexes (**1**–**4**) have been tested by MTT assay against liver carcinoma cells (HepG-2) and breast carcinoma cells (MCF-7), in comparison to the cisplatin as a positive control. The IC_{50} values estimated for the tested compounds are listed in Table 3 and Fig. 4, referred that all compounds have good activity against cell lines. In general, $[PdCl_2(HDmazo)]$ complex is significantly more potent than other complexes and free ligand with IC_{50} values 13.67 ± 1.02 μM and 9.83 ± 0.72 μM for MCF-7 and HepG-2 cells, respectively. Meanwhile, the IC_{50} values for $[PtCl_2(HDmazo)]$ complex against MCF-7 and HepG-2 cells are 16.30 ± 1.12 μM and 14.01 ± 0.89, respectively. whereas the deprotonated complexes $[M(Dmazo)_2]$ (**3**) and (**4**) showed good activity but lowest than complexes (**1**) and (**2**). The IC_{50} value of $[Pd(Dmazo)_2]$ is 26.78 ± 1.41 μM and 22.32 ± 1.19 against the MCF-7 and HepG-2 cells, respectively. Whereas the IC_{50} value of $[Pt(Dmazo)_2]$ is 27.93 ± 1.39 μM and 25.43 ± 1.04 against the MCF-7 and HepG-2 cells, respectively.

There are a number of explanations for why metal complexes are more cytotoxic than the free azo dye ligand:

i. The enhancement of molecular planarization upon chelation of ligands to metal ions.
ii. The electron delocalization system is extended by the formation of metallo-cycles.
iii. Additional electrostatic interactions between complex and negatively charged bio-macromolecule fragments of metal ions [40].

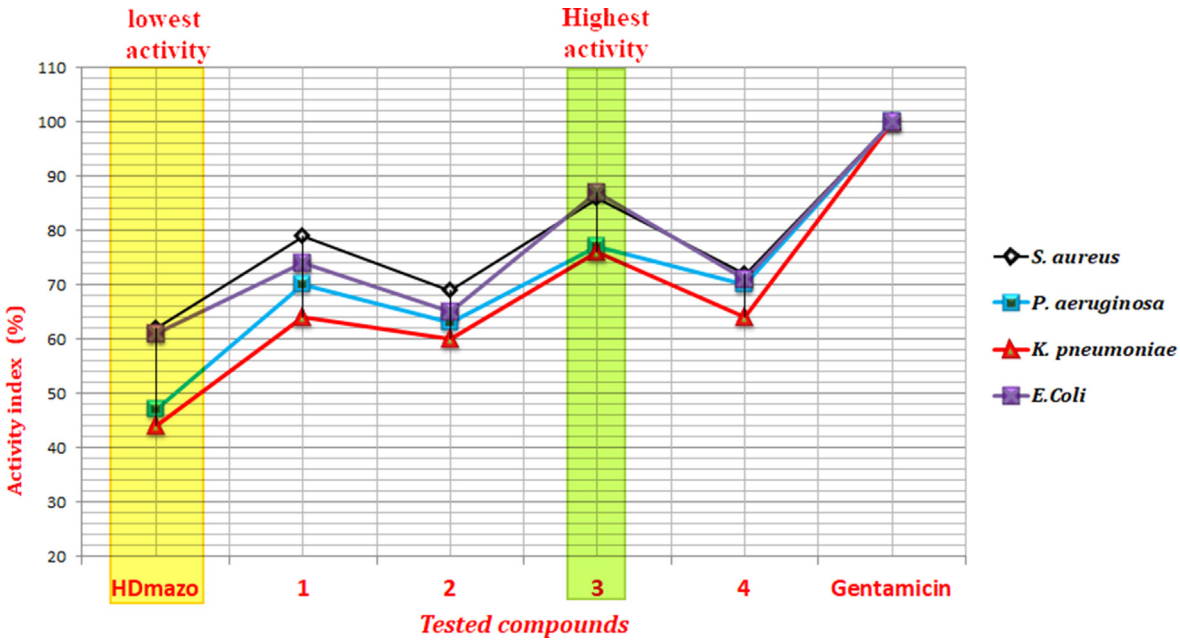

Fig. 3 Activity index of Schiff base ligand and its complexes.

Table 2 MIC (μg/ mL) values of the free ligand and its complexes.

Compounds	MIC (μg/ mL)			
	Escherichia coli	*Staphylococcus aureus*	*Klebsiella pneumoniae*	*Pseudomonas aeruginosa*
HDmazo	**200**	**200**	**300**	**200**
1	**100**	**80**	**80**	**100**
2	**100**	**100**	**80**	**100**
3	**150**	**100**	**100**	**150**
4	**150**	**150**	**100**	**150**
Gentamicin	**80**	**80**	**40**	**80**
Amoxicillin	**100**	**100**	**100**	**100**

Table 3 IC_{50} values of the tested compounds against MCF-7 and HepG-2 cell line.

Comps.	IC_{50} value (μM)	
	MCF-7	HepG-2
HDmazo	30.39 ± 0.597	34.69 ± 0.636
1	13.67 ± 1.02	9.83 ± 0.72
2	16.30 ± 1.12	14.01 ± 0.89
3	26.78 ± 1.41	22.32 ± 1.19
4	27.93 ± 1.39	25.43 ± 1.04
Cis-platin	3.45 ± 0.42	4.05 ± 0.22

Additionally, the metal ion has the ability to selectively interact with a range of bioactive substrates, leading to a number of cytotoxic mechanisms in the cancer cells that prevent them from proliferating [41].

3.7. Molecular docking

The binding style of the Erlotinib showed an energy-binding of −8.75 kcal/ mol against EGFR tyrosine kinase. The 4-aminequinazoline moiety produced five Pi-Alkyl interactions with Leu694, Leu820, Ala719 and one hydrogen bond with Met769, additionally the bis(2-methoxyethoxy) moiety binding with Cys773 by two hydrogen bonds, moreover the 3-ethynylphenyl formed one Pi-Alkyl interaction with Lys721 (Fig. 5).

The binding mode of the candidate free ligand (**HDmazo**) exhibited an energy binding of −6.86 kcal/ mol against EGFR tyrosine kinase. Which creating six Pi-Alkyl interactions with Leu764, Leu820, Lys721 and Val702, additionally interacted with Leu764 and Phe832 by two hydrogen bonds with a distance of 2.76 and 2.05 Å (Fig. 6).

The binding mode of the candidate complexes (**1**) and (**2**) exhibited an energy binding of −6.75 kcal/ mol and −6.57 kcal/ mol against EGFR tyrosine kinase, respectively. Complex (**1**) creating five Pi-Alkyl and Pi-cation interactions

Table 4 DG(kcal/mol) of the free ligand and its complexes against (EGFR tyrosine kinase) target site PDB ID: 4HJO.

Ligand	RMSD value (Å)	Affinity score (kcal/mol)	Interactions	
			H.B	Pi-interactions
Erlotinib	1.26	−8.75	4	6
HDmazo	1.05	−6.86	2	6
1	1.35	−6.75	2	5
2	1.48	−6.57	1	2
3	1.01	−8.03	1	7
4	1.28	−9.12	1	13

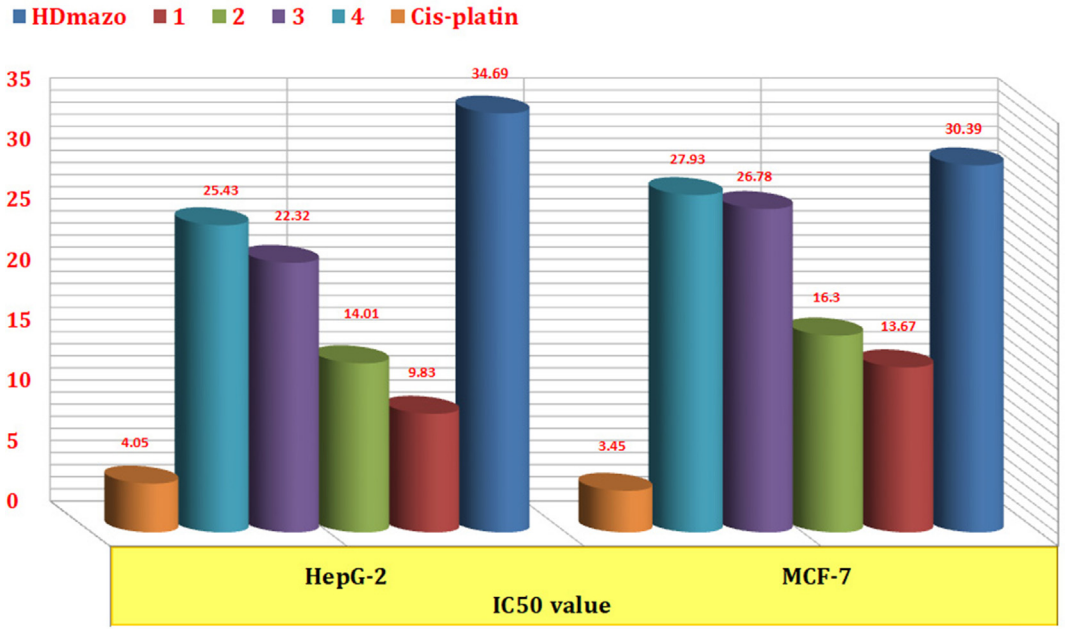

Fig. 4 Histogram of IC_{50} values of the tested compounds against MCF-7 and HepG-2 cell line.

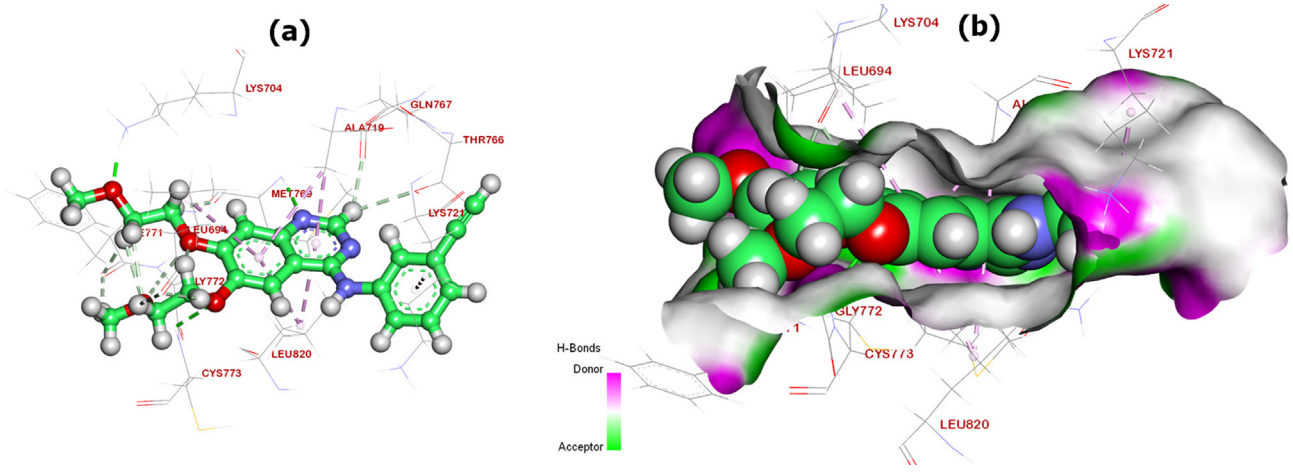

Fig. 5 (**a**) standard drug (Erlotinib) *docked in* EGFR tyrosine kinase, hydrogen bonds (green) and the π-bonding are characterized in purple lines, (**b**) Mapping surface of Erlotinib occupying the active pocket of EGFR tyrosine kinase.

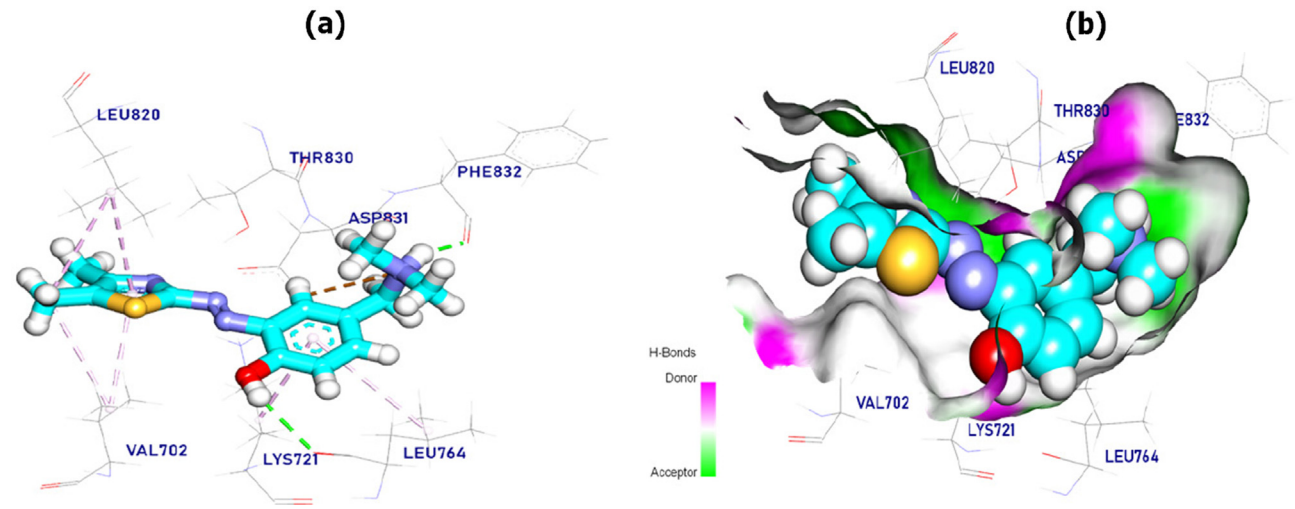

Fig. 6 (**a**) HDmazo ligand *docked in* EGFR tyrosine kinase, hydrogen bonds (green), the pi interactions are represented in purple lines (**b**) Mapping surface of HDmazo ligand occupying the active pocket of EGFR tyrosine kinase.

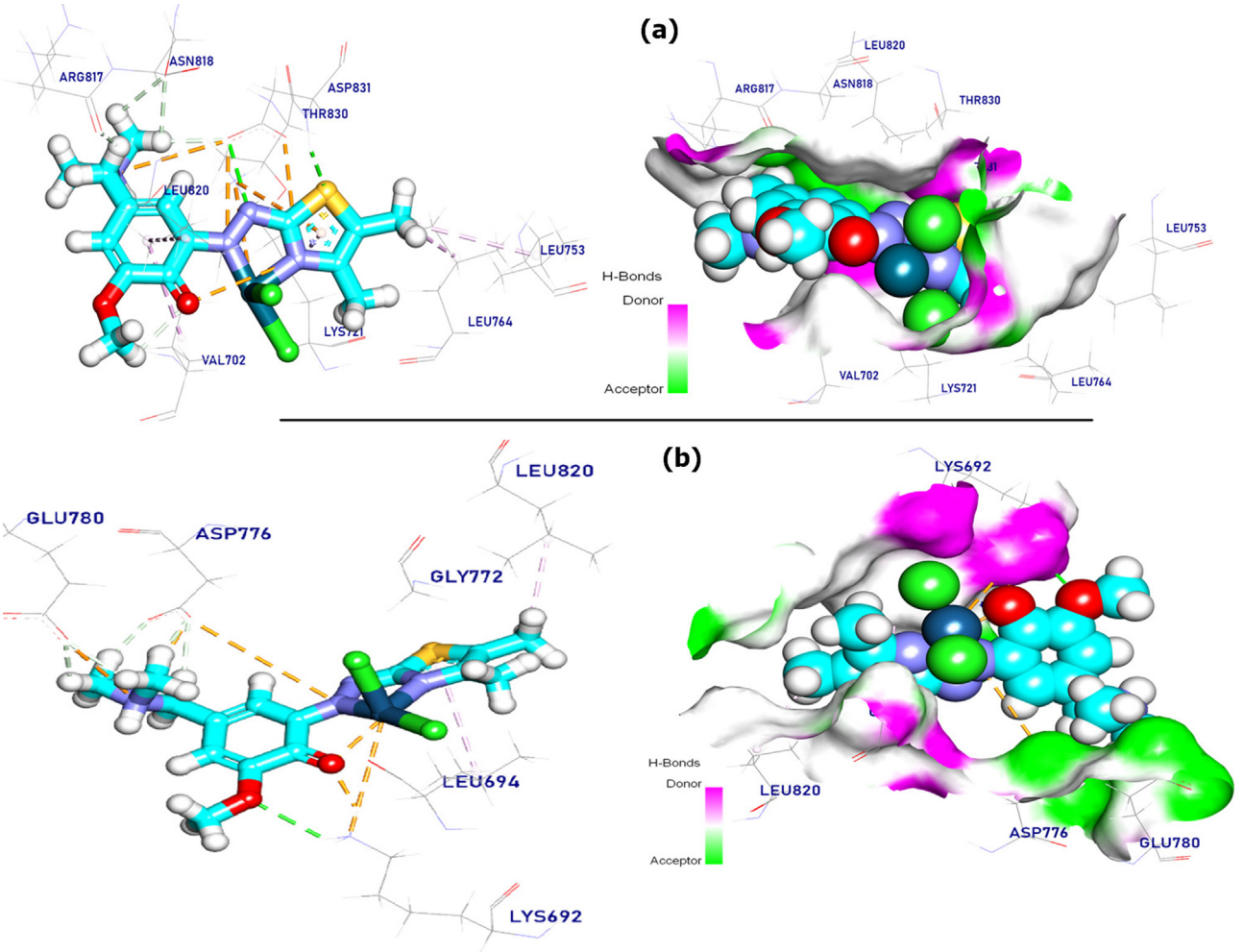

Fig. 7 Complex 1 (a) and complex 2 (b) docked in EGFR tyrosine kinase, hydrogen bonds (green) and the pi interactions are represented in purple lines with Mapping surface occupying the active pocket of EGFR tyrosine kinase.

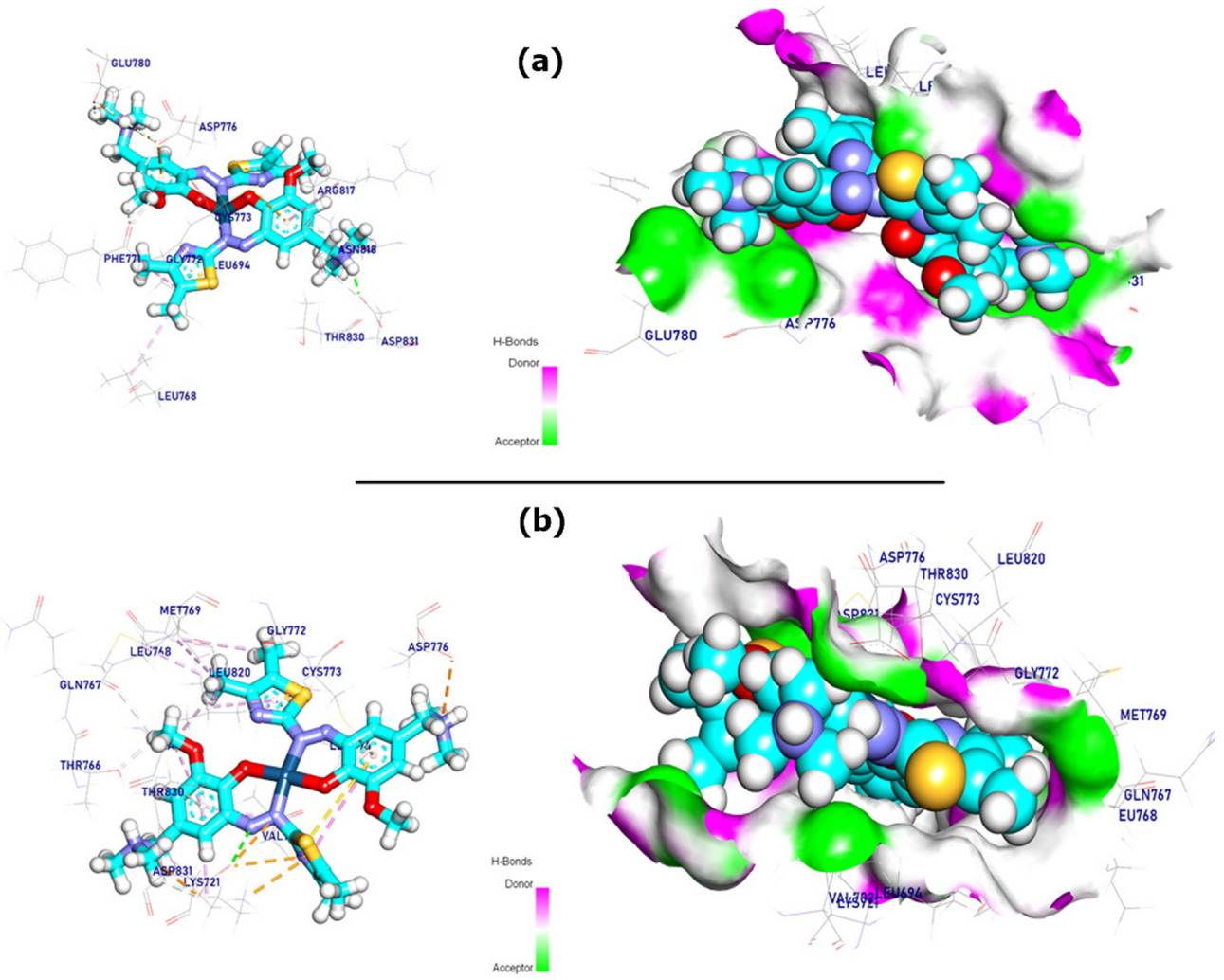

Fig. 8 Complex 3 (a) and complex 4 (b) docked in EGFR tyrosine kinase, hydrogen bonds (green) and the pi interactions are represented in purple lines with mapping surface occupying the active pocket of EGFR tyrosine kinase.

with Leu753, Lys721, Leu820, Leu764, and Val702 and two hydrogen bonds with Asp831(Fig. 7**a**), whereas complex (**2**) was interacted by two Pi-Alkyl interactions with Leu694 and Leu820 and one hydrogen bond with Lys692 with distance of 2.72 Å (Fig. 7**b**).

The binding mode of the candidate complexes **3** and **4** exhibited an energy binding of −8.03 kcal/ mol and −9.12 kcal/ mol against EGFR tyrosine kinase, respectively. Complex **3** was interacted by seven Pi-Alkyl, Pi-anion and Pi-sulfur interactions with Arg817, Leu694, Cys773, Leu768, Asp776, additionally interacted with Asp831 by one hydrogen bond with distance of 2.06 Å (Fig. 8**a**). While complex **4** was created thirteen Pi-Alkyl and Pi-cation interactions with Leu820, Leu694, Met769, Ala719, Val702, Leu768 and Asp831. Moreover, formed one hydrogen bond with Asp831 with bond length 2.95 Å (Fig. 8**b**).

4. Conclusion

A series of biologically active azo dye ligand (HDmazo) has been synthesized by predictable diazoium coupling reaction at 0–5 °C. The synthesized azo dye ligands were utilized for metallization with Pd (II) and Pt(II) in1:1 or 1:2 stoichiometric ratio as ligand: metal in present or without present base. The structural established by spectral (FTIR, ^{1}H NMR, ^{13}C NMR, mass), elemental analysis, and molar conductivity studies. On the basis of physicochemical and spectroscopic data, the square planner geometry. The results of biological activity indicated that azo dye ligand and its complexes (**1**–**4**) have good activity against the pathogenic bacteria, and the [Pd(Dmazo)$_2$] (**3**) showed a highest activity than the other compounds. Further, all compounds have good activity against MCF-7 and HepG-2 cell lines, and [PdCl$_2$(HDmazo)] is significantly more potent with IC_{50} values 13.67 ± 1.02 µM and 9.83 ± 0.72 µM for MCF-7 and HepG-2 cells, respectively. Moreover, the molecular docking studies support the experimental data.

Declaration of Competing Interest

The authors declare that they have no known competing financial interests or personal relationships that could have appeared to influence the work reported in this paper.

Acknowledgment

The authors extend their appreciation to the Deputyship for Research & Innovation, Ministry of Education in Saudi Arabia for funding this research work through the project no. (IFKSURG-2-983).

Appendix A. Supplementary material

Supplementary data to this article can be found online at https://doi.org/10.1016/j.jscs.2023.101619.

References

[1] P.G. Demingos, N.M. Balzaretti, A.R. Muniz, First-principles study of carbon nanothreads derived from five-membered heterocyclic rings: thiophene, furan and pyrrole, Phys. Chem. Chem. Phys. 23 (3) (2021) 2055–2062.
[2] M. Pervaiz, S. Sadiq, A. Sadiq, U. Younas, A. Ashraf, Z. Saeed, M. Zuber, A. Adnan, Azo-Schiff base derivatives of transition metal complexes as antimicrobial agents, Coord. Chem. Rev. 447 (2021).
[3] A.S. Waheeb, H.A. Kadhim Kyhoiesh, A.W. Salman, K.J. Al-Adilee, M.M. Kadhim, Metal complexes of a new azo ligand 2-[2′-(5-nitrothiazolyl) azo]-4-methoxyphenol (NTAMP): synthesis, spectral characterization, and theoretical calculation, Inorg. Chem. Commun. 138 (2022).
[4] H.A.K. Kyhoiesh, K.J. Al-Adilee, Synthesis, spectral characterization, antimicrobial evaluation studies and cytotoxic activity of some transition metal complexes with tridentate (N, N, O) donor azo dye ligand, Results Chem. 3 (2021).
[5] A.S. Waheeb, K.J. Al-Adilee, Synthesis, characterization and antimicrobial activity studies of new heterocyclic azo dye derived from 2-amino- 4,5- dimethyl thiazole with some metal ions, Mater. Today: Proceedings 42 (2021) 2150–2163.
[6] S.H. Alotaibi, A.S. Radwan, Y.K. Abdel-Monem, M.M. Makhlouf, Synthesis, thermal behavior and optical characterizations of thin films of a novel thiazole azo dye and its copper complexes, Spectrochim. Acta, Part A 205 (2018) 364–375.
[7] K.J. Al-Adilee, A. Shaimaa, Synthesis and spectral properties studies of novel hetrocyclic mono azo dye derived from thiazole and pyridine with some transition complexes, Orient. J. Chem. 33 (4) (2017) 1–14.
[8] A.S. Waheeb, K.J. Al-Adilee, A.S. Al-Janabi, R. Shanmuganathan, M.M. Kadhim, Synthesis, characterization, cytotoxic, and computational studies of new complexes (copper and cadmium), J. Mol. Struct. 1267 (2022).
[9] A.M. Khedr, H. El-Ghamry, M.A. Kassem, F.A. Saad, N. El-Guesmi, Novel series of nanosized mono- and homobi-nuclear metal complexes of sulfathiazole azo dye ligand: synthesis, characterization, DNA-binding affinity, and anticancer activity, Inorg. Chem. Commun. 108 (2019).
[10] J. Lu, X. Tong, X. He, A mercury ion-selective electrode based on a calixarene derivative containing the thiazole azo group, J. Electroanal. Chem. 540 (2003) 111–117.
[11] M. Tunçel, S. Serin, Synthesis and characterization of new azo-linked Schiff bases and their cobalt(II), copper(II) and nickel(II) complexes, Transition Met. Chem. 31 (6) (2006) 805–812.
[12] E. İspir, The synthesis, characterization, electrochemical character, catalytic and antimicrobial activity of novel, azo-containing Schiff bases and their metal complexes, Dyes Pigm. 82 (1) (2009) 13–19.
[13] M. Tunçel, S. Serin, Synthesis and characterization of Copper (II), Nickel(II) and Cobalt(II) complexes with azo-linked schiff base ligands, Synth. React. Inorg. M. 35 (3) (2005) 203–212.
[14] J. Sahoo, S.K. Paidesetty, Biological investigation of novel metal complexes of 2-amino-4-substituted phenylthiazole Schiff bases, J. Taibah Univ. Medical Sci. 13 (2) (2018) 142–155.
[15] I.N. Witwit, Z.Y. Motaweq, H.M. Mubark, Synthesis, Characterization, and Biological Efficacy on new mixed ligand complexes based from azo dye of 8-hydroxy quinoline as a primary ligand and imidazole as a secondary ligand with some of transition metal ions, J. Pharm. Sci. Res. 10 (12) (2018) 3074.
[16] S.M. Mahdi, A.K. Ismail, Preparation and Identification of new azo-schiff base ligand (NASAR) and its divalent transition metal Complexes, J. Pharm. Sci. Res. 10 (9) (2018) 2175–2178.
[17] A.-N.M.A. Alaghaz, M.E. Zayed, S.A. Alharbi, Synthesis, spectral characterization, molecular modeling and antimicrobial studies of tridentate azo-dye Schiff base metal complexes, J. Mol. Struct. 1084 (2015) 36–45.
[18] M. Gaber, H.A. El-Ghamry, S.K. Fathalla, Synthesis, structural identification, DNA interaction and biological studies of divalent Mn, Co and Ni chelates of 3-amino-5-mercapto-1,2,4-triazole azo ligand, Appl. Organomet. Chem. 34 (8) (2020) e5678.
[19] A.W. Bauer, D.M. Perry, W.M.M. Kirby, Single-Disk Antibiotic-Sensitivity Testing of Staphylococci: An Analysis of Technique and Results, AMA Arch. Intern. Med. 104 (2) (1959) 208–216.
[20] C.H. Tan, D.S.Y. Sim, M.P. Heng, S.H. Lim, Y.Y. Low, T.S. Kam, K.S. Sim, Evaluation of DNA Binding and Topoisomerase I Inhibitory Activities of 16'-Decarbomethoxydihydrovoacamine from *Tabernaemontana corymbosa*, ChemSelect 5 (47) (2020) 14839–14843.
[21] A.S.M. Al-Janabi, T.A. Yousef, M.E.A. Al-Doori, R.A. Bedier, B.M. Ahmed, Palladium(II)-salicylanilide complexes as antibacterial agents: Synthesis, spectroscopic, structural characterization, DFT calculations, biological and in silico studies, J. Mol. Struct. 1246 (2021).
[22] D.-Q. Chen, C.-H. Guo, H.-R. Zhang, D.-P. Jin, X.-S. Li, P. Gao, X.-X. Wu, X.-Y. Liu, Y.-M. Liang, A metal-free transformation of alkynes to carbonyls directed by remote OH group, Green Chem. 18 (15) (2016) 4176–4180.
[23] M.M. Salih, A.M. Saleh, A.S. Hamad, A.S. Al-Janabi, Synthesis, spectroscopic, anti-bacterial activity, molecular docking, ADMET, toxicity and DNA binding studies of divalent metal complexes of pyrazole-3-one azo ligand, J. Mol. Struct. 1264 (2022) 133252.
[24] N. Venugopal, G. Krishnamurthy, H.S. Bhojyanaik, P. Murali Krishna, Synthesis, spectral characterization and biological studies of Cu (II), Co (II) and Ni (II) complexes of azo dye ligand containing 4-amino antipyrine moiety, J. Mol. Struct. 1183 (2019) 37–51.
[25] A.S. Al-Janabi, W.A. Al-Jumaili, L.J. Al-Hayaly, S.A. Al-Jibori, H. Schmidt, C. Wagner, G. Hogarth, Synthesis and in vitro cytotoxicity studies of Pd(II) and Pt(II) acetamide complexes: Molecular structures of trans-[PdCl2(bzmta)2].DMF (bzmta = 2-acetylamino-6-methylbenzothiazole) and cis-[PtCl2 (bzta)2].2DMF (bzta = 2-acetylaminobenzothiazole), Polyhedron 185 (2020).
[26] C.-Y. Shi, E.-J. Gao, S. Ma, M.-L. Wang, Q.-T. Liu, Synthesis, crystal structure, DNA-binding and cytotoxicity in vitro of novel *cis*-Pt(II) and *trans*-Pd(II) pyridine carboxamide complexes, Bioorg. Med. Chem. Lett. 20 (24) (2010) 7250–7254.
[27] H.H. Nguyen, C.D. Le, C.T. Pham, T.N. Trieu, A. Hagenbach, U. Abram, Ni(II), Pd(II) and Cu(II) complexes with *N*-(dialkylthiocarbamoyl)-*N*′-picolylbenzamidines: Structure and activity against human MCF-7 breast cancer cells, Polyhedron 48 (1) (2012) 181–188.

[28] A.S.M. Al-Janabi, W.A. Al-Jumaili, T.S. Saeed, O.A. Abd, E. Sinn, Pd(II) and Pt(II) complexes with N-(1,3-benzothiazol-2-yl) acetamide ligands, spectroscopic characterization, DFT computational and in-vitro cytotoxicity studies, Mater. Today: Proc. 43 (2021) 977–985.
[29] E.N. Al-Sabawi, A.S. Al-Janabi, H.M. Jerjes, Synthesis and Spectroscopic study of Pd(II)- Salicylaldoxime complexes with amine ligands, Tikrit J. Pure Sci. 26 (3) (2021) 26–34.
[30] Y.S. El-Sayed, M. Gaber, R.M. Fahmy, S. Fathallah, Characterization, theoretical computation, DNA-binding, molecular docking, antibacterial, and antioxidant activities of new metal complexes of (E)-1-([1H-1,2,4-triazol-3-yl]diazenyl)naphthalen-2-ol, Appl. Organomet. Chem. 36 (5) (2022) e6628.
[31] Y. El-Sayed, M. Gaber, N. El-Wakeil, A. Abdelaziz, A. El-Nagar, Metal complexes of azo mesalamine drug: Synthesis, characterization, and their application as an inhibitor of pathogenic fungi, Appl. Organomet. Chem. 35 (8) (2021) e6290.
[32] A. Abdelaziz, M. Gaber, N. El-Wakiel, Y.S. El-Sayed, Ag(I), In (III), and Sn (II) chelates of azo mesalamine drug: Characterization, DFT studies, molecular docking and biological evaluation, Appl. Organomet. Chem. 37 (2) (2023) e6944.
[33] A.S. Faihan, M.R. Hatshan, M.M. Kadhim, A.S. Alqahtani, F. A. Nasr, A.M. Saleh, S.A. Al-Jibori, A.S. Al-Janabi, Promising bio-active complexes of platinum(II) and palladium(II) derived from heterocyclic thiourea: Synthesis, characterization, DFT, molecular docking, and anti-cancer studies, J. Mol. Struct. 1252 (2022) 132198.
[34] B. Tweedy, Plant extracts with metal ions as potential antimicrobial agents, Phytopathology 55 (1964) 910–914.
[35] N. Raman, Synthesis, Structural Characterization, Redox and Antimicrobial Studies of Schiff Base Copper(II), Nickel(II), Cobalt(II), Manganese(ii), Zinc(II) and Oxovanadium(ii) Complexes derived from benzil and 2-Aminobenzyl Alcohol, Pol. J. Chem. 76 (2002) 1085–1094.
[36] P.H. Viale, The American Cancer Society's Facts & Figures: 2020 Edition, J. Adv. Pract. Oncol. 11(2) (2020) 135-136.
[37] O. Cauli, Oxidative stress and cognitive alterations induced by cancer chemotherapy drugs: a scoping review, Antioxidants 10 (7) (2021) 1116.
[38] R.F.M. Elshaarawy, I.M. Eldeen, E.M. Hassan, Efficient synthesis and evaluation of bis-pyridinium/bis-quinolinium metallosalophens as antibiotic and antitumor candidates, J. Mol. Struct. 1128 (2017) 162–173.
[39] M.Y. Alfaifi, S.E.I. Elbehairi, H.S. Hafez, R.F.M. Elshaarawy, Spectroscopic exploration of binding of new imidazolium-based palladium(II) saldach complexes with CT-DNA as anticancer agents against HER2/neu overexpression, J. Mol. Struct. 1191 (2019) 118–128.
[40] A.R.E. Mahdy, M.Y. Alfaifi, M.S. El-Gareb, N. Farouk, R.F.M. Elshaarawy, Design, synthesis, and physicochemical characterization of new aminothiohydantoin Schiff base complexes for cancer chemotherapy, Inorg. Chim. Acta 526 (2021).
[41] W.N. El-Sayed, J. Alkabli, K. Althumayri, R.F.M. Elshaarawy, L.A. Ismail, Azomethine-functionalized task-specific ionic liquid for diversion of toxic metal ions in the aqueous environment into pharmacological nominates, J. Mol. Liq. 322 (2021).